Arab J Geosci (2015) 8:8601–8613
DOI 10.1007/s12517-015-1831-6

ORIGINAL PAPER

Landslide susceptibility mapping and factor effect analysis using frequency ratio in a catchment scale: a case study from Garuwa sub-basin, East Nepal

Prabin Kayastha

Received: 29 March 2014 / Accepted: 6 February 2015 / Published online: 27 February 2015

Abstract For assessing landslide susceptibility, the spatial distribution of landslides in the field is essential. The landslide inventory map is prepared on the basis of historical information of individual landslide events from different sources such as previously published reports, satellite imageries, aerial photographs and interview with local inhabitants. Then, the distribution of landslides in the study area is verified with field surveys. However, the selection of contributing factors for modelling landslide susceptibility is an inhibit task. The previous studies show that the factors are chosen as per availability of data. This paper documents the landslide susceptibility mapping in the Garuwa sub-basin, East Nepal using frequency ratio method. Nine different contributing factors are considered: slope aspect, slope angle, slope shape, relative relief, geology, distance from faults, land use, distance from drainage and annual rainfall. To analyse the effect of contributing factors, the landslide susceptibility index maps are generated four times using (a) topographical factors and geological factors, (b) topographical factors, geological factors and land use, (c) topographical factors, geological factors, land use and drainage and (d) all nine causative factors. By comparing with the pre-existing landslides, the fourth case (considering all nine causative factors) yields the best success rate accuracy, i.e. 81.19 %, which is then used to produce the final landslide susceptibility zonation map. Then, the final landslide susceptibility map is validated through chi-square test. The standard chi-square value with 3 degrees of freedom at the 0.001 significance level is 16.3, whereas the calculated chi-square value is 7,125.79. Since the calculated chi-square value is greater than the standard chi-square value, it can be concluded that the landslide susceptibility map is considered as statistically significant. Moreover, the results show that the predicted susceptibility levels are found to be in good agreement with the past landslide occurrences.

Keywords Landslide susceptibility · Frequency ratio · Factor effect · Garuwa sub-basin · Nepal

P. Kayastha (✉)
Department of Hydrology and Hydraulic Engineering, Vrije Universiteit Brussel Pleinlaan 2, 1050 Brussels, Belgium
e-mail: pkayasth@vub.ac.be

P. Kayastha
Mountain Risk Engineering Unit, Tribhuvan University Kirtipur, Kathmandu, Nepal

P. Kayastha
Attic Consulting Service Thamel, Kathmandu, Nepal

Introduction

Extending from Afghanistan to Myanmar, the Himalaya region is inherently fragile and susceptible to landslides as a result of its rugged mountain topography, soft soil cover, high-intensity monsoon precipitation and weak nature of the geological structures (Upreti and Dhital 1996; Chalise 2001). Landslide problems in this region are further aggravated by anthropogenic factors such as deforestation, unsound agricultural practices, haphazard settlement and unplanned developmental works (Upreti and Dhital 1996; Kayastha et al. 2010). Every year, especially during the monsoon season, a lot of damage to life and property is caused by the landslides in this region. In Nepal alone, the average annual number of deaths caused by landslides and floods from 1983 to 2009 was about 280 and in 1993 was as high as 1,336 (DWIDP 2010). In order to control or mitigate problems caused by mass movements, systematic studies of landslides including inventory mapping, susceptibility mapping, hazard mapping and risk assessment have to be carried out (Kayastha et al. 2012). Within the last few decades, numerous attempts at landslide susceptibility and hazard and risk mapping have been made throughout the world mainly due to increasing awareness of the socio-economic impacts as well as increasing pressure of urbanisation on environment (Aleotti and Chowdhury 1999). Overviews of the different landslide susceptibility and hazard mapping are given by Varnes (1984), Carrara et al. (1995), Soeters and van Westen (1996), Aleotti and Chowdhury (1999), Guzzetti et al. (1999) and Wang et al. (2005). The most common approaches for assessing landslide susceptibility and hazard can be grouped into five categories (Carrara et al. 1995; Soeters and van Westen 1996; Aleotti and Chowdhury 1999; Guzzetti et al. 1999; Wang et al. 2005), namely: (1) direct geomorphological mapping; (2) analysis of landslide inventories; (3) heuristic methods; (4) statistical methods including fuzzy logic and artificial neural networks; and (5) process based conceptual modelling.

Different researchers have used statistical models to obtain the landslide susceptibility/hazard map in different parts of the world. Statistical methodologies can be broadly divided into bivariate and multivariate. In the bivariate methodologies, the weight value for each class of different factors responsible for landslide is obtained on the basis of relationship between past landslides and each class of different causative factors (van Westen 1994). These weight values can be obtained from different statistical methodologies such as general instability index (Carrara et al. 1978), frequency index (Parise and Jibson 2000), surface percentage index (Uromeihy and Mahdavifar 2000), information value method (Yin and Yan 1988), statistical index method (van Westen 1997), weighting factor (Çevik and Topal 2003), certainty factor (Chung and Fabbri 1993), conditional analysis (Carrara et al. 1995), weights of evidence (van Westen 1993), frequency ratio (Lee and Min 2001), probability analysis (Tien Bui et al. 2013) and landslide susceptibility analysis (Süzen and Doyuran 2004).

In this study, the bivariate frequency ratio methodology is applied for obtaining the weight values. The main advantage of using bivariate frequency ratio methodology is that the weight values measure, directly or in a weighted form, the relative or absolute abundance of landslide area or number in different classes. Hence, this methodology is used by different researchers in different parts of world such as Lee and Min (2001) in Yongin, Korea; Lee (2004) in Janghung area, Korea; Lee et al. (2004) and Choi et al. (2012) in Boun, Korea; Lee and Dan (2005) in Lai Chau Province, Vietnam; Lee and Talib (2005) and Lee and Lee (2006) in Gangneung, Korea; Lee and Pradhan (2006) in Penang, Malaysia; Lee and Sambath (2006) in Damrei Romel area, Cambodia; Lee and Pradhan (2007) in Selangor, Malaysia; Vijith and Madhu (2007, 2008) in Kerala, India; Akgun et al. (2008) in Findikli, Turkey; Jadda et al. (2009) in Marzan Abad, Iran; Oh et al. (2009) in Pechabun area, Thailand; Yilmaz (2009) in Tokat, Turkey; Yilmaz and Keskin (2009) in Sebinkarahisar, Turkey; Ehret et al. (2010) in the Xiangxi catchment, Three Gorges Reservoir area, China; Oh et al. (2010) in Pemalang, Indonesia; Poudyal et al. (2010) in Panchthar, Nepal; Pradhan (2010) in the Cameron catchment, Malaysia; Pradhan and Lee (2010a) in Klang valley, Malaysia; Pradhan and Lee (2010b) in Penang Island, Malaysia; Pradhan and Youssef (2010) in Cameron, Malaysia; Yilmaz (2010) in Koyulhisar, Turkey; Akinci et al. (2011) at Samsun, Turkey; Intarawichi and Dasananda (2011) in the Mae Chaem watershed, Thailand; Jadda et al. (2011) in the Central Alborz, Iran; Mezughi et al. (2011) in Gerik-Jeli, Malaysia; Yalcin et al. (2011) in Trabzon, Korea; Akgun (2012) in İzmir, Turkey; Lepore et al. (2012) in Puerto Rico; Reis et al. (2012) in Rize Province, Turkey; and Sujatha et al. (2013) in Tevankarai Ar sub-watershed, Kodaikkanal, India.

This paper summarises the outcomes of a landslide susceptibility mapping study in the Garuwa sub-basin, East Nepal (Fig. 1a) using the bivariate statistical frequency ratio method and also deals with the effect analysis of different causative factors responsible for landslide occurrences.

The objectives of the present study are to (i) prepare a landslide inventory maps and maps of the causative factors of landslides; (ii) compute the weight values for each factor based on the frequency ratio; (iii) analyse the effect of each of these factors responsible for landslide occurrences; (iv) determine the most successful combination of different causative factors that generates the best landslide susceptibility map; and (v) check the statistical significance of the obtained landslide susceptibility map using a chi-square test.

Study area

The Garuwa sub-basin (Fig. 1a) lies in the Ilam and Jhapa Districts of the Mechi Zone in eastern Nepal. This sub-basin lies between latitudes 26° 39′ 30″ to 26° 50′ 30″ N and longitudes 87° 44′ 00″ to 87° 58′ 00″ E. It covers an area about 228 km^2 and has a more or less triangular shape. The altitude varies from 120 m near Domukha in the south to 1,520 m near Soktim in the northeast of the sub-basin (Fig. 1b). The Kankai River is the main watercourse, and the Mai Khola, the Garuwa Khola and the Lodiya Khola are its major tributaries (*Khola* means a stream in the Nepali language) (Fig. 1b).

The Garuwa sub-basin lies mainly in Siwaliks Range. However, a small part of the sub-basin in the southern part lies in the Terai region, whereas a small part in the northeast part lies in the Mahabharat Range. The Main Boundary Thrust (MBT) separates the Mahabharat Range from the Siwaliks Range.

There are two climatic zones, i.e. a subtropical zone (150–1,200 m) and a warm temperate humid zone (above 1,200 m), in this sub-basin. The average temperature is 20 to 35 °C in the subtropical zone whereas 10 to 30 °C in the warm temperate humid zone. The annual rainfall varies from 2,250 to 2, 650 mm (Table 1). A detail description of this sub-basin can be found in Kayastha (2012).

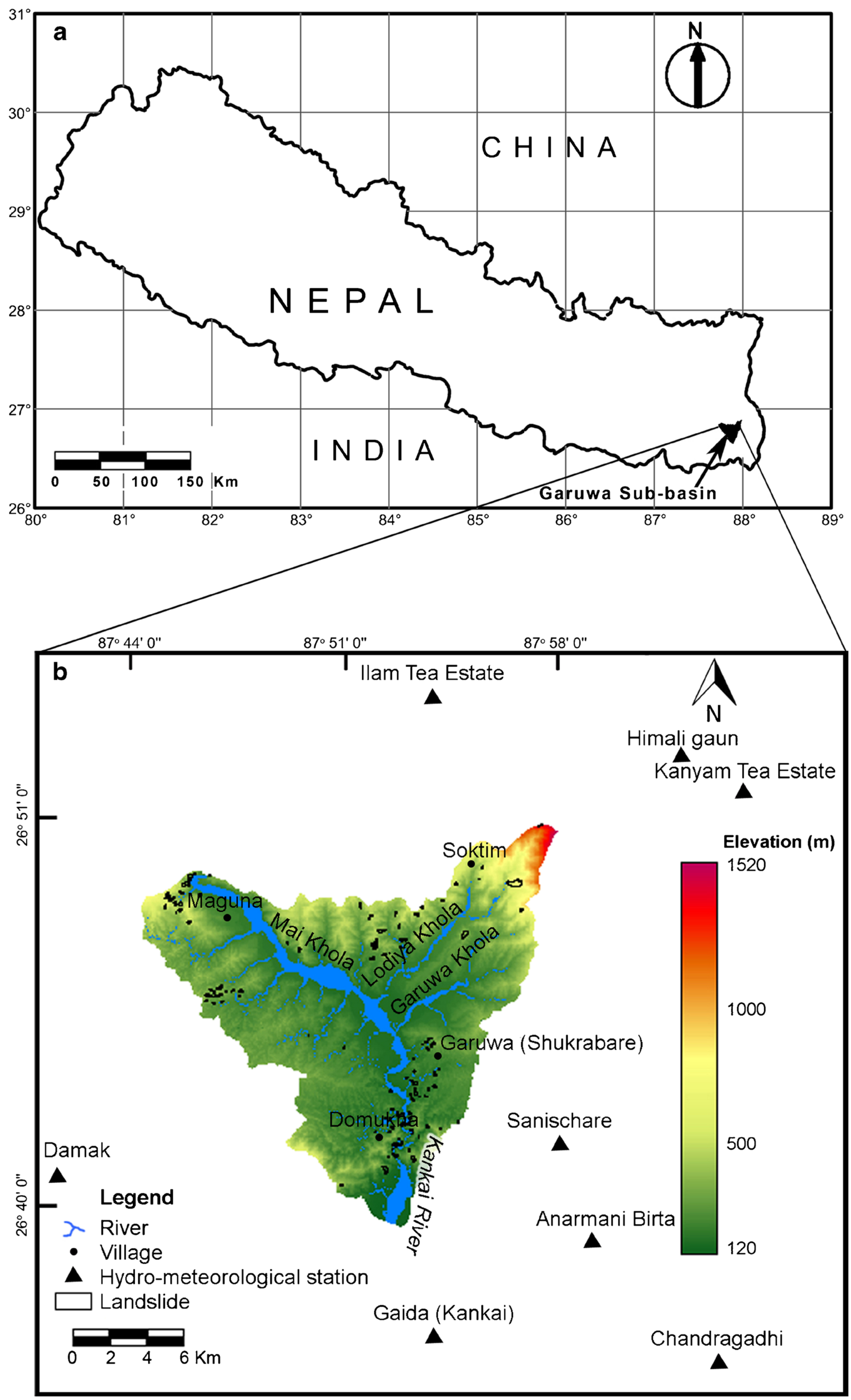

Fig. 1 **a** Location of the study area and **b** digital elevation model (DEM) of the study area with rivers, hydro-meteorological stations and landslide distributions

Materials

Different thematic data on causative factors are needed to prepare a landslide susceptibility map. These data are collected from different sources. For instance, digital elevation contour lines, land cover maps and aerial photos are collected from the Department of Survey, Government of Nepal. A geological map (1:250,000 scale) was prepared by Pradhan et al. (2006) obtained from the Department of Mines and Geology, Government of Nepal. Daily rainfall data from 1985 to 2007, recorded at eight hydro-meteorological stations situated inside or just outside of the study area (Fig. 1b), are collected from the Department of Hydrology and Meteorology, Government of Nepal. Data on landslides are collected by field reconnaissance in April 2010.

These data sources are used to prepare thematic digital maps using GIS software. All maps are raster based with a cell size of 20 m×20 m. Detail descriptions for each data layer are described below.

Landslide inventory map

For assessing landslide susceptibility, the spatial distribution of landslides in the field is essential (Deoja et al. 1991). Landslide inventories are the simplest form of landslide mapping (Guzzetti et al. 1999). In order to prepare the landslide inventory map, the researcher should collect historical information of individual landslide events from different sources such as previously published reports, satellite imageries, aerial photographs and interview with local inhabitants. Then, the distribution of landslides in the study area should be verified with field surveys. The study revealed 136 landslides in the Garuwa sub-basin (Fig. 1b), covering an area of about 1.75 km^2 or about 0.77 % of the study area. During field visit on 2010 April, it was found that most of these slides were already stabilised and consisted mainly of shallow soil or rock slides, plane or wedge failures and rotational slides.

Table 1 Average annual rainfall (mm) recorded at the hydro-meteorological stations from 1985 to 2007 (source: Department of Hydrology and Meteorology, Government of Nepal)

Station no.	Station name	Altitude (m) above mean sea level	Longitude	Latitude	Average annual rainfall (mm)
1407	Ilam Tea Estate	1,300	87° 54′	26° 55′	1,715
1408	Damak	163	87° 42′	26° 40′	2,345
1409	Anarmani Birta	122	87° 59′	26° 38′	2,487
1410	Himali Gaun	1,654	88° 02′	26° 53′	2,404
1412	Chandragadhi	120	88° 03′	26° 34′	2,281
1415	Sanischare	168	87° 58′	26° 41′	2,762
1416	Kanyam Tea Estate	1,678	88° 04′	26° 52′	3,147
1421	Gaida (Kankai)	143	87° 54′	26° 35′	2,589

Topographic factors

From the digital elevation contours with intervals of 20 m, a digital elevation model (DEM) of the study area (Fig. 1b) was prepared. From this DEM, topographical thematic data layers such as slope aspect, slope angle, slope shape (curvature) and relative relief were prepared.

Slope aspect

The direction of maximum slope of the terrain surface gives the slope aspect. In this study, slope aspect was divided into nine classes: (i) north (N), (ii) northeast (NE), (iii) east (E), (iv) southeast (SE), (v) south (S), (vi) southwest (SW), (vii) west (W), (viii) northwest (NW) and (ix) flat. Almost one third of the study area lies in the flat aspect (Table 2).

Slope angle

Slope angle is one of the most important parameter which influences the stability of slope (Terzaghi and Peck 1967). In this study, a map of slope angle was generated from the DEM and classified into five different classes: (i) flat to gentle slope (<15°), (ii) moderate slope (15–25°), (iii) fairly moderate slope (25–35°), (iv) steep slope (35–45°) and (v) very steep slope (>45°). Previous studies show that slope gradients between 25° and 45° are prone to failure in the Nepal Himalayas (Deoja et al. 1991; Kayastha et al. 2010). However, landslides also occur on gentler as well as on moderate slopes in this sub-basin (Table 2). In this study area, almost half of the study area lies in the flat to gentle slope (<15°).

Slope shape (curvature)

The study area was classified according to slope curvature values: (i) convex, (ii) concave and (iii) straight (planar). Generally, concave slopes are considered as potentially unstable as they concentrate water at the lowest point and contribute to develop adverse hydrostatic pressure, whereas convex slopes are more stable as they disperse the runoff more equally down the slope (Stocking 1972). Contrary to this, straight slopes are found more stable than the concave or convex slopes in this study area (Table 2).

Relative relief

The maximum height dispersion of a terrain normalised by its length or area is known as relative relief (Oguchi 1997). In this study, relative relief was computed as the difference

Table 2 Spatial relationships between each class of causative factors and observed landslides and resulting frequency ratio

Causative factors	A^*_{ij}		A_{ij}		W_{ij}
	(Pixels)	(%)	(Pixels)	(%)	
Topographic factors					
Slope aspect					
North	177	4.04	37,092	6.51	0.62
Northeast	225	5.13	42,619	7.48	0.68
East	363	8.28	42,429	7.45	1.11
Southeast	719	16.40	53,339	9.36	1.76
South	297	6.78	53,139	9.32	0.73
Southwest	714	16.29	44,620	7.83	2.10
West	386	8.81	40,782	7.16	1.23
Northwest	303	6.91	46,090	8.09	0.85
Flat	1,199	27.36	209,784	36.81	0.74
Slope angle					
0–15°	1,072	24.46	278,542	48.88	0.50
15–25°	692	15.79	104,479	18.33	0.86
25–35°	1,252	28.56	101,843	17.87	1.61
35–45°	834	19.03	56,120	9.85	1.95
>45°	533	12.16	28,910	5.07	2.42
Slope curvature					
Concave	2,178	49.69	222,353	39.02	1.28
Planar (straight)	285	6.50	126,748	22.24	0.29
Convex	1,920	43.81	220,793	38.74	1.13
Relative relief					
<25 m/ha	150	3.42	169,650	29.77	0.11
25–50 m/ha	1,194	27.24	200,757	35.23	0.77
50–100 m/ha	2,569	58.61	184,582	32.39	1.82
>100 m/ha	470	10.72	14,905	2.62	4.20
Geological factors					
Geology					
Quartzites, phyllites, schists	58	1.32	34,233	6.01	0.22
Banded gneiss	515	11.75	10,747	1.89	6.49
Middle Siwaliks	1,657	37.81	231,468	40.62	0.93
Lower Siwaliks	1,825	41.64	93,500	16.41	2.57
Gravel beds	326	7.44	94,493	16.58	0.45
Recent alluvium	2	0.05	53,950	9.47	0.00
River beds	0	0.00	51,503	9.04	0.00
Distance from faults					
<1 km	876	19.99	101,702	17.85	1.12
>1 km	3,507	80.01	468,192	82.15	0.97
Land use					
Cultivation and built-up area	530	12.09	170,432	29.91	0.40
Tea plantation	0	0.00	7,760	1.36	0.00
Forest	3,731	85.12	335,598	58.89	1.45
Grassland	2	0.05	3,964	0.70	0.07
Bush	4	0.09	856	0.15	0.61
Sandy area	0	0.00	41,339	7.25	0.00
Barren land	116	2.65	3,474	0.61	4.46
Water body	0	0.00	6,471	1.14	0.00
Hydrological and climatic factors					
Distance from drainage					
<25 m	1,896	43.26	208,851	36.65	1.18
25–50 m	1,149	26.21	146,337	25.68	1.02
50–100 m	869	19.83	132,432	23.24	0.85
>100 m	469	10.70	82,274	14.44	0.74
Annual rainfall					
2,250–2,400 mm/year	1,481	33.79	148,294	26.02	1.30
2,400–2,550 mm/year	1,460	33.31	330,993	58.08	0.57
>2,550 mm/year	1,442	32.90	90,607	15.90	2.09
Total	**4,383**		**569,894**		

between maximum and minimum altitudes (m) per hectare of land. Relative relief was divided into the four classes: (i) <25 m/ha, (ii) 25–50 m/ha, (iii) 50–100 m/ha and (iv) >100 m/ha.

Geological factors

Geology is one of the most influential factors, which plays an important role in slope stability. As stated previously, Pradhan et al. (2006) prepared the geological map of the study area. The digital geological map (Fig. 2) was prepared on the basis of the geological map of Pradhan et al. (2006) and field observations.

The lithological units of the Garuwa sub-basin belong to the Neogene-Quaternary Group and Lesser Himalayan Group (Pradhan et al. 2006). The Neogene-Quaternary Group consists of river beds, recent alluvium, Lower Siwaliks, Middle Siwaliks and Upper Siwaliks. Quaternary alluvial deposits are found in the intermontain valleys of the Mai River, Garuwa River and Kankai River. These deposits consist of alluvial fans, terraces and bars made up of gravels, sands and silts. The Lower Siwaliks are fine-grained, hard, grey sandstones interbedded with purple and green shales. The Middle Siwaliks consist of fine- to medium-grained arkosic pebbly sandstones with rare grey to dark grey clays and occasionally with silty sandstones and conglomerates. The Upper Siwaliks consist of coarse boulder conglomerates with irregular beds of sandstones and thin intercalations of yellow, brown, and grey

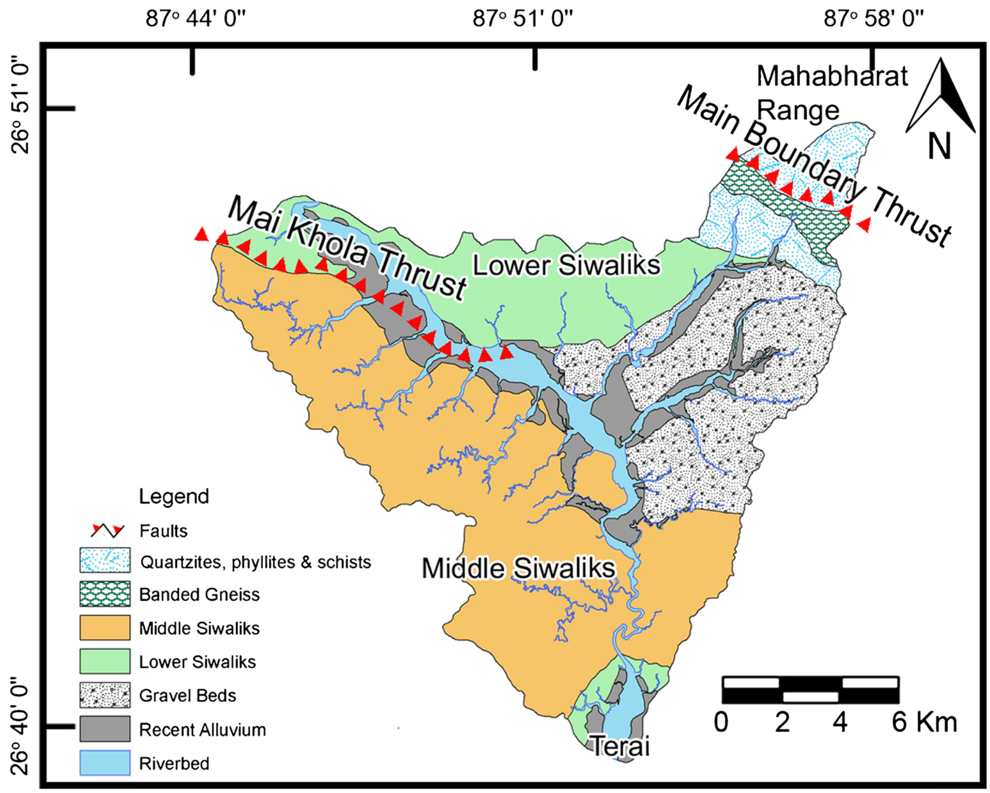

Fig. 2 Geological map of the study area, modified after Pradhan et al. (2006)

sandy clays. The Lesser Himalayan group consists of quartzites, grey-green phyllites, grey metasandstones, grey garnetiferous schists with dark grey-green amphibolites and banded gneisses.

Active thrusts increase landslide susceptibility because rocks near a fault are weaker, due to intense shearing (Leir et al. 2004). Active thrusts such as the MBT and the Mai Khola Thrust (MKT) are also found in the study area (Fig. 2). The MBT separates the Lesser Himalayan rocks from the Siwaliks like in other parts of the Nepal Himalaya. The MKT is covered at many places by alluvial deposits of the Mai Khola. A digital map of distance from active faults was prepared using the Euclidian distance method and classified into two classes: (i) <1 km and (ii) >1 km.

Land use

Land use is one of most important factor for slope instability. Based on a land cover map prepared by the Department of Survey, Government of Nepal and field study, eight land use classes were considered, as shown in Fig. 3, i.e. (i) cultivation and built-up areas, (ii) tea plantation, (iii) forest, (iv) grass land, (v) bush, (vi) sandy area, (vii) barren land and (viii) water body. Almost 32 % of the study area is used for cultivation or tea plantation with few built-up areas, and 7 % of the study area is covered by the sandy area whereas 59 % of the study area is covered by the forest.

Hydrological and climatic factors

Runoff also plays an important role in slope instability. In this sub-basin, landslides occur frequently on stream banks (Fig. 1b). Hence, in order to see the effect of runoff on landsliding, a digital thematic distance from drainage map was prepared using the Euclidian distance method. Then, the study area was classified into four classes: (i) <25 m, (ii) 25–50 m, (iii) 50–100 m and (iv) >100 m. Almost 37 % of the study area lies in <25 m.

Landslide processes are closely related with rainfall in Nepal (Dhital et al. 1993; Gabet et al. 2004; Dahal and Hasegawa 2008). Annual total rainfall from 1985 to 2007 observed in eight hydro-meteorological stations (Table 1 and Fig. 1b) situated just outside of the study area was used to prepare a rainfall map, classified in three classes: (i) 2,250–2,400 mm/year, (ii) 2,400–2,550 mm/year and (iii)>2,550 mm/year. Almost three fifth of the study area annually receives 2,400–2,550-mm rainfall.

Methodology

Frequency ratio

A landslide susceptibility map is prepared by combining causative factors with quantitatively defined weight values. In the present study, the frequency ratio method (Lee and Min 2001)

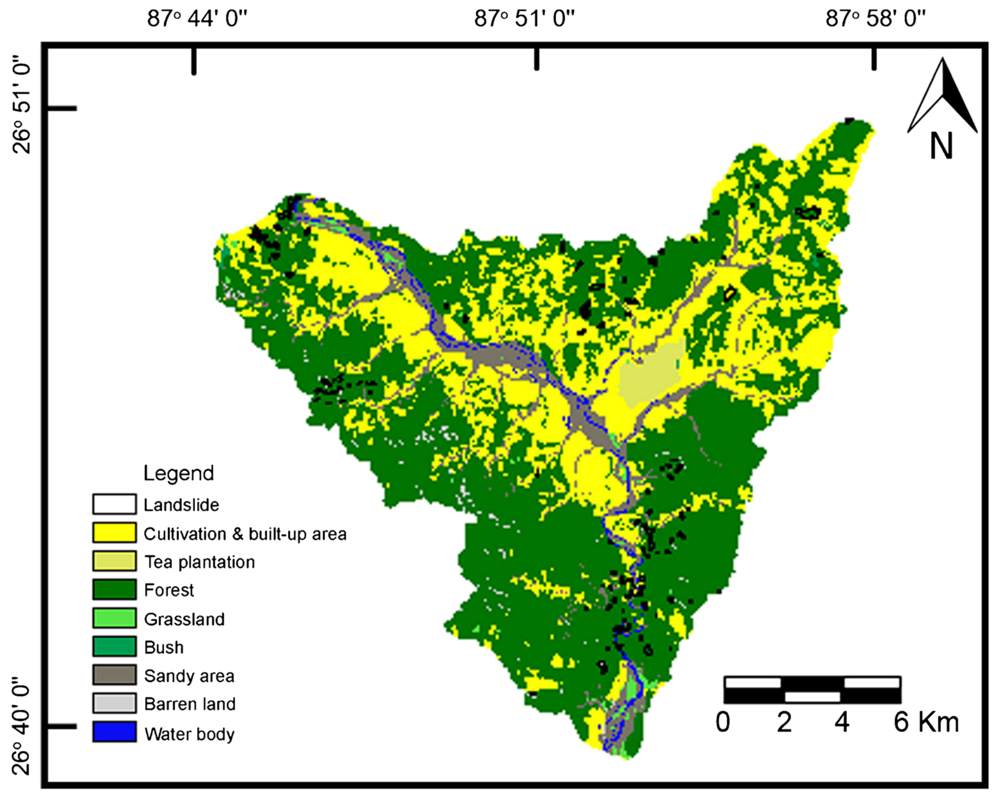

Fig. 3 Land cover map of the study area

is used in which a weight value for a parameter class is obtained as follows:

$$W_{ij} = \frac{f^*_{ij}}{\overline{f}^*_{ij}} = \frac{A^*_{ij}}{A^*} \times \frac{A - A^*}{A_{ij} - A^*_{ij}} \quad (1)$$

where W_{ij} is the weight value or frequency ratio of class i of parameter j, $f^*_{ij} = A^*_{ij}/A^*$ is the frequency of observed landslides in class i of parameter j, $\overline{f}^*_{ij} = \left(A_{ij} - A^*_{ij}\right)/(A - A^*)$ is the frequency of non-observed landslides in class i of parameter j, A^*_{ij} is the area of landslides in a class i of parameter j, A_{ij} is the area of class i of parameter j, A^* is the total area of landslides in the study area and A is the total area of the study area.

Relationship between landslide and causative factors

If the frequency ratio is greater than 1, the relationship between landslides and the factors is high and, if the ratio is less than 1, the relationship between landslide and the factors is low.

In case of the relationship between landslide occurrence and slope aspect, landslides are more abundant on southwest-facing and southeast-facing slopes, whilst the frequency of landslides is lowest on north, northeast-facing, south and northwest-facing slopes. The main reason behind this may be that the monsoon storms in Nepal enter from the east and slowly move towards the west producing a lot of precipitation in the southern slopes than northern slopes.

Previous studies show that in Nepal, flat to gentle slopes are expected to be safe from slope instability, whereas steep to very steep natural slopes are susceptible to landsliding (Kayastha et al. 2010, 2012). The results in Table 2 show that for slope angles less than 25°, the frequency ratio is less than 1, which indicates a low probability of landslide occurrence, whilst for slope angles more than 25°, the frequency ratio is greater than 1, which indicates a high probability of landslide occurrence.

For slope curvature (shape), the frequency ratio is larger than 1 for both convex and concave slopes and less than 1 for straight slopes. This may be due to retention of more water by convex or concave slopes after heavy rainfall, which increases soil water pressures and reduces shear resistance (Lee and Min 2001).

In case of relative relief, the frequency ratio is larger than 1 for 50-100 m/ha and >100 m/ha classes and less than 1 for <25 m/ha and 25–50 m/ha classes. This result reveals indication of relative relief as the potential energy for mass wasting and soil erosion (Ghimire 2001).

In the case of landslide occurrence and geology, the frequency ratio is higher for the banded gneiss of the Lesser Himalaya and Lower Siwaliks, whereas the frequency ratio is lower in the river beds, recent alluvium, quartzites, phylites, schists, Upper Siwaliks and Middle Siwaliks. In this sub-basin, rocks of the Lower Siwaliks and banded gneiss are highly weathered so that these rocks are susceptible to landsliding. On the other hand, quartzites, phylites, schists, rocks of the

Table 3 Success rate accuracy and area under curve (AUC) for different cases

Sample no.	Cases	Success rate accuracy (%)	Area under curve (AUC)
1	Topographical and geological factors	77.21	0.7721
2	Topographical factors, geological factors and land use	77.96	0.7796
3	Topographical factors, geological factors, land use and drainage	78.40	0.7840
4	Topographical factors, geological factors, land use, drainage and rainfall	81.19	0.8119

Middle Siwaliks and Upper Siwaliks are moderately strong to hard in nature so that these rocks are more resistant to slope failure. The presence of a fault increases landslide susceptibility because rocks near a fault are weaker due to intense shearing (Leir et al. 2004). This is proved by the results shown in Table 2 as the frequency ratio for the distance from faults less than 1 km is more than 1.

The effect of land use is also seen in the study area. For certain land uses such as cultivation and built-up area, grassland, tea plantation, sandy area and bush, the frequency ratio is less than 1 indicating the lower probability of landslide occurrences, whereas the frequency ratio is more than 1 for barren land and forest indicating that these land uses are highly susceptible for landslide occurrences.

In the present study area, the drainage has a clear influence on landslides because the closer the drainage is the greater is the frequency ratio. At a distance of less than 25 m and 25–50 m classes, the frequency ratio is more than 1, whereas at a

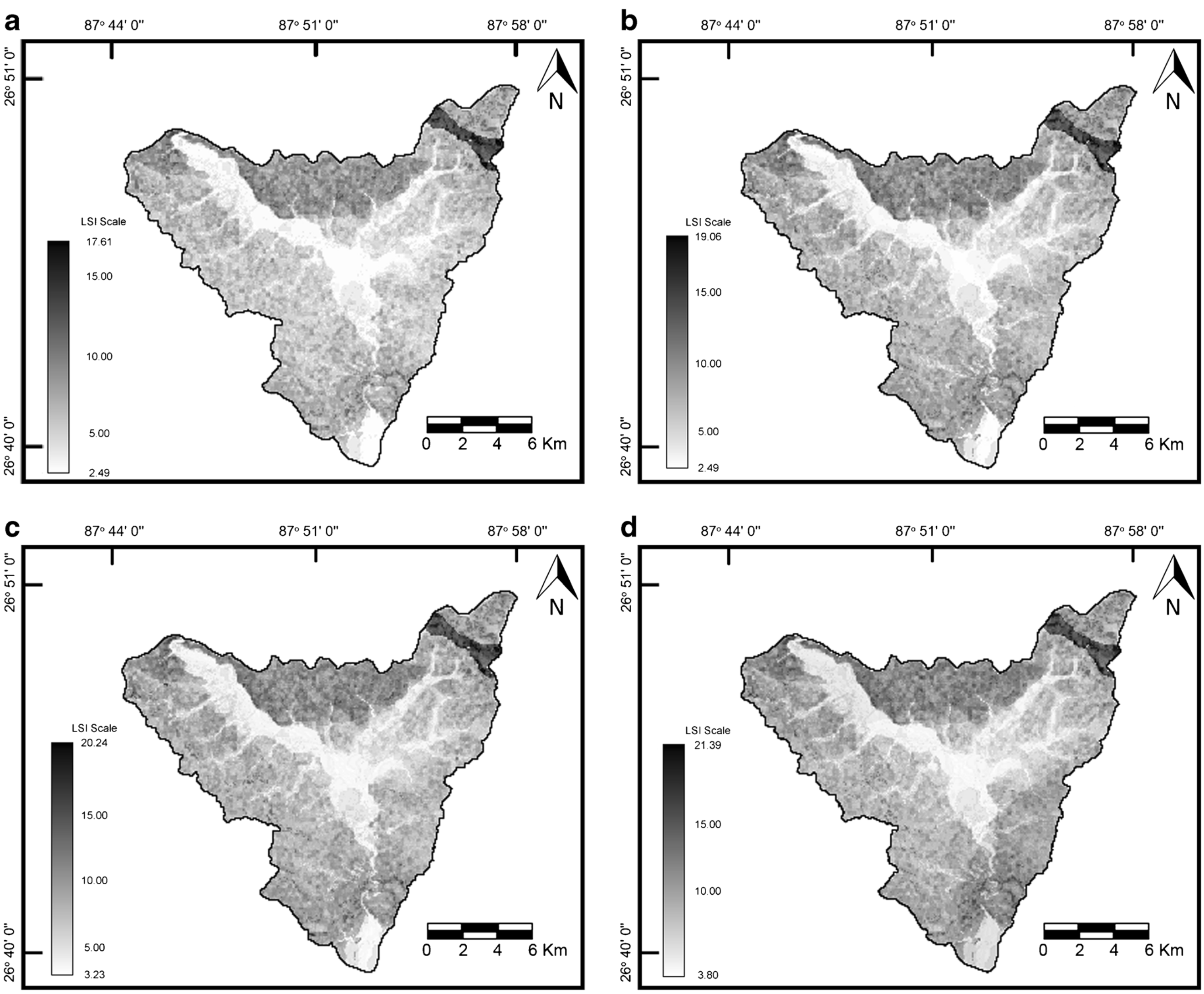

Fig. 4 Landslide susceptibility index (*LSI*) maps of the study area derived from **a** topographical and geological factors; **b** topographical factors, geological factors and land use; **c** topographical factors, geological factors, land use and drainage; and **d** topographical factors, geological factors, land use, drainage and annual rainfall

distance greater than 50 m, the frequency ratio is less than 1. This result clearly shows that there is a lower probability of landslides further away from rivers.

Rainfall also has higher influences on the initiation of landslides. For the area with annual rainfall more than 2,550 mm, the frequency ratio is higher than other areas. However, the area with annual rainfall 2,400–2,550 mm has almost 33 % of the observed landslides, but due to high area covered by this class, the frequency ratio becomes less than 1 indicating less probability of landslide occurrences in this class.

Landslide susceptibility mapping

Finally, the integration of the various causative factors and classes in a single landslide susceptibility index (LSI) is given by a procedure based on the weighted linear sum

$$\mathrm{LSI} = \sum\nolimits_{j=1}^{n} W_{ij}. \quad (2)$$

where n is the number of parameters.

The effect of the causative factors can be seen in the landslide susceptibility mapping by exclusion of causative factors during the summation stage using Eq. 2. The studies of effect analysis show how a susceptibility index map changes when the input causative factors are changed (Lee and Talib 2005; Jadda et al. 2009). The causative factors that have the most influences on the calculated landslide susceptibility index map can be identified using effect analysis. In the present study, four cases were chosen, as shown in Table 3 and Fig. 4, to see the effect of causative factors in the landslide susceptibility. Then, the success rate curve (Chung and Fabbri 1999, Kayastha et al. 2012) is obtained for each case by plotting the cumulative percentage of observed landslide occurrence against the areal cumulative percentage in decreasing LSI values as shown in Fig. 5. The area under a curve is used to assess the success accuracy qualitatively. The area under curve for four different cases is shown in Table 3. For instance, in the case of taking topographic factors and geological factors, the area under curve is 0.7721 which means that the success rate accuracy is 77.21 %, and in the case of taking all causative factors, the area under curve is 0.8119 indicating that the success rate accuracy is 81.19 %. Table 3 shows that amongst four different cases, the first three cases, such as taking (i) topographic factors and geological factors, (ii) topographic factors, geological factors and land use and (iii) topographic factors, geological factors, land use and distance from drainage, produce almost identical results for the success rates. The best result for the success rate accuracy is produced by the fourth case which considers all the causative factors. Hence, the LSI map (Fig. 4d), which is derived from considering all the causative factors, is chosen to produce the landslide susceptibility zonation map (Fig. 6).

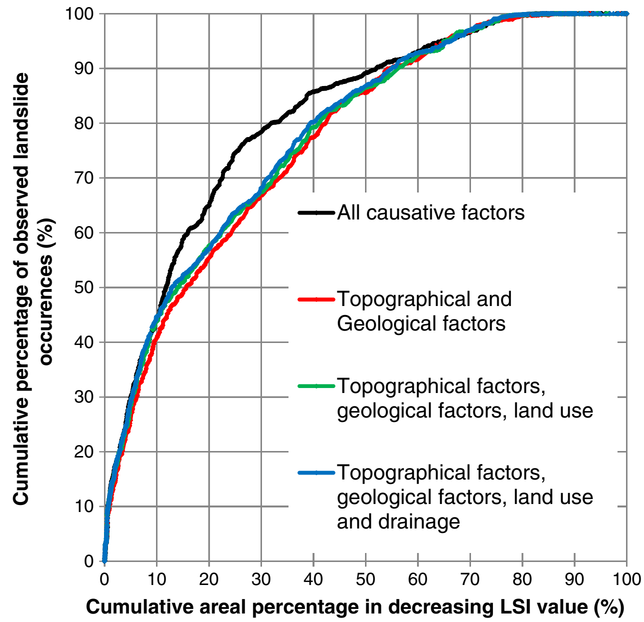

Fig. 5 Graph showing success rate curves, i.e. cumulative percentage of observed landslide occurrences versus cumulative areal percentage of decreasing LSI values

This map is categorised into low, moderate, high and very high landslide susceptible zones such that 40 % of the study area has low LSI values, 30 % of the study area has moderate LSI values, 20 % has high LSI values and the remaining 10 % of the study area has the highest LSI values (Bijukchhen et al. 2013; Kayastha et al. 2012). It shows that the very high susceptible zone occupies 44.06 % of the total landslide occurrences, whereas high, moderate and low susceptible zones cover 34.29, 14.74 and 6.91 % of the total landslides, respectively (Fig. 6 and Table 4).

For validation of a landslide susceptibility map, the computation of landslide density of each susceptibility zone is important as the landslide density assesses the overall quality of the landslide susceptibility map (Sarkar and Kanungo 2004). The results presented in Table 4 showed that the landslide density for the very high susceptible zone is 0.0339. Furthermore, landslide density values gradually declined from very high to low susceptible zones as shown in Table 4. Hence, the landslide susceptibility map reveals the existing field instability conditions.

A chi-square test also can be performed in order to test the statistical significance and effectiveness of the landslide susceptibility map (Sarkar and Kanungo 2004; Kayastha et al. 2012). For the null hypothesis, it was assumed that the presence of landslide cells in different susceptibility classes were purely due to chance. The observed number of cells with and without landslides for each of the four susceptibility classes was determined from the map (upper part of Table 5), and the

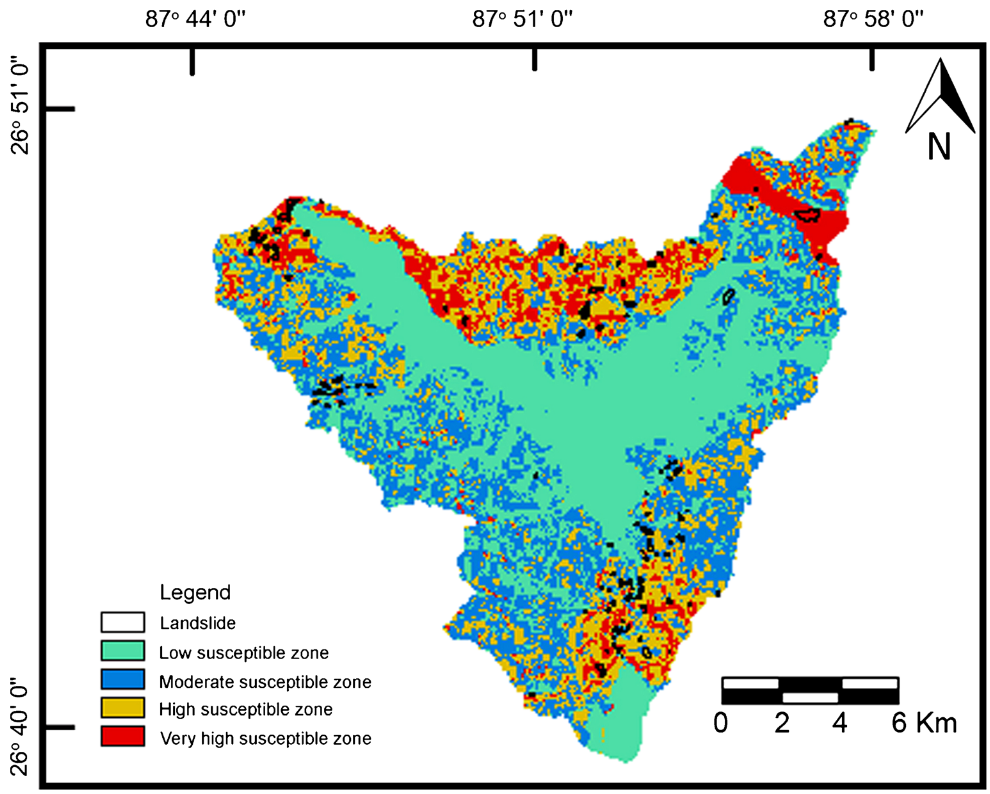

Fig. 6 Landslide susceptibility zonation map of the study area derived by using all causative factors

expected number of cells for the same was estimated from the observed values using expected probabilities (middle part of Table 5). The standard chi-square value with 3 degrees of freedom at the 0.001 significance level is 16.3. The total discrepancy, i.e. chi-square value computed for the above data, is 7,125.79 (lower part of Table 5). Since the calculated chi-square value is greater than the standard chi-square value, it can be concluded that the landslide susceptibility map is considered as statistically significant.

Conclusions

The selection of contribution factors for modelling landslide susceptibility is an inhibit task. In the present study, nine different contributing factors (slope aspect, slope angle, slope curvature, relative relief, geology, distance from faults, land cover, distance from drainage and annual rainfall) are chosen to model the landslide susceptibility using frequency ratio method. Four landslide susceptibility index maps are

Table 4 Distribution of susceptibility zones and observed landslides and resulting landslide density

Susceptibility zones	Study area		Landslide area		Landslide density
	(km^2)	(%)	(km^2)	(%)	
Low	91.2083	40.00	0.1212	6.91	0.0013
Moderate	68.4063	30.00	0.2585	14.74	0.0038
High	45.6044	20.00	0.6014	34.29	0.0132
Very high	22.8024	10.00	0.7726	44.06	0.0339
Total	228.0214	100.00	1.7537	100.00	0.0077

Table 5 Results for the chi-square test, indicating observed number of cells with or without landslide in each susceptibility zone, the corresponding expected number of cells in case landslide occurrence would be random and the resulting chi-square values

Observed number of cells					
Susceptibility zones	Low	Moderate	High	Very high	Total
Without landslide	227,654	170,322	112,476	55,059	565,511
With landslide	303	646	1,503	1,931	4,383
Total	227,957	170,968	113,979	56,990	569,894
Expected number of cells					
Susceptibility zones	Low	Moderate	High	Very high	Total
Without landslide	226,204	169,653	113,102	56,552	565,511
With landslide	1,753	1,314	877	438	4,383
Total	227,957	170,968	113,979	56,990	569,894
Chi-square value					
Susceptibility zones	Low	Moderate	High	Very high	Total
Without landslide	9.30	2.64	3.47	39.40	54.80
With landslide	1,199.56	340.27	447.61	5,083.54	7,070.99
Total	1,208.86	342.91	451.08	5,122.94	7,125.79

generated by selection of different causative factors. The results show that the landslide susceptibility index map produced by using all nine causative factors reveals the best success rate accuracy, i.e. 81.19 %, which is later used for producing the final landslide susceptibility zonation map.

The analysis shows that landslides are more abundant on southwest-facing and southeast-facing slopes, whilst the frequency of landslides is lowest on north, northeast-facing, south and northwest-facing slopes. For slope angles more than 25°, there is a high probability of landslide occurrence in this study area. The probability of landslide occurrence is higher for the banded gneiss of the Lesser Himalaya and Lower Siwaliks than the river beds, recent alluvium, quartzites, phylites, schists, Upper Siwaliks and Middle Siwaliks. In this sub-basin, rocks of the Lower Siwaliks and banded gneiss are highly weathered so that these rocks are susceptible to landsliding, whereas quartzites, phylites, schists, rocks of the Middle Siwaliks and Upper Siwaliks are moderately strong to hard in nature so that these rocks are more resistant to slope failure. The land uses such as barren land and forest are highly susceptible for landslide occurrences. At a distance of less than 25 and 25–50 m from drainage, there is high susceptibility for landslide occurrences. Rainfall also has higher influences on the initiation of landslides.

The landslide susceptibility zonation map reveals that 10 % of the study area lies on the very high susceptible zone which predicts 44.06 % of the past landslides. Likewise, 20 % of the study area is situated on high susceptible zone and predicts 34.29 % of the past landslides. In addition, results from the landslide density analysis and chi-square test prove that landslide susceptibility map is statistically significant. Hence, this landslide susceptibility map is trustworthy for future land use planning and disaster management planning.

Acknowledgments The author would like to thank two anonymous reviewers for constructive suggestions to improve the quality of paper. The author also extends his profound thanks to Prof. Dr. Florimond De Smedt of Vrije Universiteit Brussel, Belgium and Prof. Dr. Megh Raj Dhital of Tribhuvan University, Nepal for their supervision of this research work. The author is also indebted to the Department of Survey, Government of Nepal for providing digital data; the Department of Mines and Geology, Government of Nepal for providing geological map; and the Department of Hydrology and Meteorology, Government of Nepal for sharing hydro-meteorological data. Special thanks go to the Flemish Inter-University Council (VLIR), Belgium for research funding.

References

Akgun A (2012) A comparison of landslide susceptibility maps produced by logistic regression, multi-criteria decision, and likelihood ratio methods: a case study at İzmir, Turkey. Landslides 9:93–106

Akgun A, Dag S, Bulut F (2008) Landslide susceptibility mapping for a landslide-prone area (Findikli, NE of Turkey) by likelihood-frequency ratio and weighted linear combination models. Environ Geol 54:1127–1143

Akinci H, Doğan S, Kiliçoğlu C, Temiz MS (2011) Production of landslide susceptibility map of Samsun (Turkey) City Center by using frequency ratio method. Int J Phys Sci 6(5):1015–1025

Aleotti P, Chowdhury R (1999) Landslide hazard assessment: summary review and new perspectives. Bull Eng Geol Environ 58(1):21–44

Bijukchhen SM, Kayastha P, Dhital MR (2013) A comparative evaluation of heuristic and bivariate statistical modelling for landslide susceptibility mappings in Ghurmi–Dhad Khola, east Nepal. Arab J Geosci 6(8):2727–2743. doi:10.1007/s12517-012-0569-7

Carrara A, Catalano E, Sorriso-Valvo M, Reali C, Orso I (1978) Digital terrain analysis for land evaluation. Geol Appl Idrogeol 13:69–117

Carrara A, Cardinali M, Guzzeti F, Reichenbach P (1995) GIS technology in mapping landslide hazard. In: Carrara A, Guzzetti F (eds) Geographical information systems in assessing natural hazards. Kluwer Academic Publishers, Dordrecht, pp 135–175

Çevik E, Topal T (2003) GIS-based landslide susceptibility mapping for a problematic segment of the natural gas pipeline, Hendek (Turkey). Environ Geol 44:949–962

Chalise SR (2001) An introduction to climate, hydrology, and landslide hazards in the Hindu Kush–Himalayan region. In: Tianchi L, Chalise SR, Upreti BN (eds) Landslide hazard mitigation in the Hindu Kush-Himalayas. ICIMOD, Kathmandu, Nepal, pp 51–62

Choi J, Oh H-J, Lee H-J, Lee C, Lee S (2012) Combining landslide susceptibility maps obtained from frequency ratio, logistic regression, and artificial neural network models using ASTER images and GIS. Eng Geol 124:12–23

Chung CF, Fabbri AG (1993) Representation of geoscience information for data integration. Nat Resour Res 2(2):122–139

Chung CF, Fabbri AG (1999) Probabilistic prediction models for landslide hazard mapping. Photogramm Eng Remote Sens 65(12):1389–1399

Dahal RK, Hasegawa S (2008) Representative rainfall thresholds for landslides in the Nepal Himalaya. Geomorphology 100:429–443

Deoja BB, Dhital MR, Thapa B, Wagner A (1991) Mountain risk engineering handbook. ICIMOD, Kathmandu, Nepal, p 875

Dhital MR, Khanal N, Thapa KB (1993) The role of extreme weather events, mass movements, and land-use changes in increasing natural hazards. Workshop proceedings: causes of the recent damage incurred in South-Central Nepal, July 19–21, ICIMOD, Kathmandu, Nepal, pp.123

DWIDP (Department of Water Induced Disaster Prevention) (2010) Annual disaster review 2009. Ministry of Irrigation, Government of Nepal, Kathmandu, p 24

Ehret D, Rohn J, Dumperth C, Eckstein S, Ernstberger S, Otte K, Rudolph R, Wiedenmann J (2010) Frequency ratio analysis of mass movements in the Xiangxi catchment, Three Gorges reservoir area, China. J Earth Sci 21(6):824–834

Gabet EJ, Burbank DW, Putkonen JK, Pratt-Sitaula B, Ohja T (2004) Rainfall thresholds for landsliding in the Himalayas of Nepal. Geomorphology 63:131–143

Ghimire M (2001) Geo-hydrological hazard and risk zonation of Banganga watershed using GIS and remote sensing. J Nepal Geol Soc 23:99–110

Guzzetti F, Carrara A, Cardinali M, Reichenbach P (1999) Landslide hazard evaluation: a review of current techniques and their application in a multi-scale study, Central Italy. Geomorphology 31:181–216

Intarawichi N, Dasananda S (2011) Frequency ratio model based landslide susceptibility mapping in lower Mae Chaem watershed, Northern Thailand. Environ Earth Sci 64:2271–2285

Jadda M, Shafri HZM, Mansor SB, Sharifikia M, Pirasteh S (2009) Landslide susceptibility evaluation and factor effect analysis using probabilistic-frequency ratio model. Eur J Sci Res 33(4):654–668

Jadda M, Shafri HZM, Mansor SB (2011) PFR model and GiT for landslide susceptibility mapping: a case study from Central Alborz, Iran. Nat Hazards 57:395–412

Kayastha P (2012) Application of fuzzy logic approach for landslide susceptibility mapping in Garuwa sub-basin, East Nepal. Front Earth Sci 6(4):420–432

Kayastha P, De Smedt F, Dhital MR (2010) GIS based landslide susceptibility assessment in Nepal Himalaya: a comparison of heuristic and statistical bivariate methods. In: Malet JP, Glade T, Casagli N (eds) Mountain risks: bringing science to society. CERG Editions, France, pp 121–128

Kayastha P, Dhital MR, De Smedt F (2012) Landslide susceptibility mapping using the weight of evidence method in the Tinau watershed, Nepal. Nat Hazards 63(2):479–498

Lee S (2004) Application of likelihood ratio and logistic regression models to landslide susceptibility mapping using GIS. Environ Manag 34(2):223–232

Lee S, Dan NT (2005) Probabilistic landslide susceptibility mapping in the Lai Chau province of Vietnam: focus on the relationship between tectonic fractures and landslides. Environ Geol 48:778–787

Lee S, Lee M-J (2006) Detecting landslide location using KOMPSAT 1 and its application to landslide-susceptibility mapping at the Gangneung area, Korea. Adv Space Res 38:2261–2271

Lee S, Min K (2001) Statistical analysis of landslide susceptibility at Yongin, Korea. Environ Geol 40:1095–1113

Lee S, Pradhan B (2006) Probabilistic landslide hazards and risk mapping on Penang Island, Malaysia. J Earth Syst Sci 115(6):661–672

Lee S, Pradhan B (2007) Landslide hazard mapping at Selangor, Malaysia using frequency ratio and logistic regression models. Landslides 4:33–41

Lee S, Sambath T (2006) Landslide susceptibility mapping in the Damrei Romel area, Cambodia using frequency ratio and logistic regression models. Environ Geol 50:847–855

Lee S, Talib JA (2005) Probabilistic landslide susceptibility and factor effect analysis. Environ Geol 47:982–990

Lee S, Choi J, Woo I (2004) The effect of spatial resolution on the accuracy of landslide susceptibility mapping: a case study in Boun, Korea. Geosci J 8(1):51–60

Leir M, Michell A, Ramsay S (2004) Regional landslide hazard susceptibility mapping for pipelines in British Columbia. Geo-engineering for the society and its environment. 57th Canadian geotechnical conference and 5th joint CGS-IAH conference, October 24–27, 2004, Old Quebec, Canada, 1–9

Lepore C, Kamal SA, Shanahan P, Bras RL (2012) Rainfall-induced landslide susceptibility zonation of Puerto Rico. Environ Earth Sci 66:1667–1681

Mezughi TH, Akhir JM, Rafek AG, Abdullah I (2011) Landslide susceptibility assessment using frequency ratio model applied to an area along the E-W Highway (Gerik-Jeli). Am J Environ Sci 7(1):43–50

Oguchi T (1997) Drainage density and relative relief in humid steep mountains with frequent slope failure. Earth Surf Process Landf 22:107–120

Oh H-J, Lee S, Chotikasathien W, Kim CH, Kwon JH (2009) Predictive landslide susceptibility mapping using spatial information in the Pechabun area of Thailand. Environ Geol 57:641–651

Oh H-J, Lee S, Soedradjat GM (2010) Quantitative landslide susceptibility mapping at Pemalang area, Indonesia. Environ Geol 60:1317–1328

Parise M, Jibson RW (2000) A seismic landslide susceptibility rating of geologic units based on analysis of characteristics of landslides triggered by the 17 January, 1994 Northridge, California earthquake. Eng Geol 58:251–270

Poudyal CP, Chang C, Oh H, Lee S (2010) Landslide susceptibility maps comparing frequency ratio and artificial neural networks: a case study from the Nepal Himalaya. Environ Earth Sci 61:1049–1064

Pradhan B (2010) Landslide susceptibility mapping of a catchment area using frequency ratio, fuzzy logic and multivariate logistic regression approaches. J Indian Soc Remote Sens 38:301–320

Pradhan UMS, KC SB, Subedi DN, Sharma SR, Khanal RP, Tripathi GN (2006) Geological map of petroleum exploration block-10 Biratnagar, Eastern Nepal. Department of Mines and Geology, Kathmandu, Nepal

Pradhan B, Lee S (2010a) Landslide susceptibility assessment and factor effect analysis: backpropagation artificial neural networks and their comparison with frequency ratio and bivariate logistic regression modeling. Environ Model Softw 25:747–759

Pradhan B, Lee S (2010b) Delineation of landslide hazard areas on Penang island, Malaysia, by using frequency ratio, logistic regression, and artificial neural network models. Environ Earth Sci 60: 1037–1054

Pradhan B, Youssef AM (2010) Manifestation of remote sensing data and GIS on landslide hazard analysis using spatial-based statistical models. Arab J Geosci 3:319–326

Reis S, Yalcin A, Atasoy M, Nisanci R, Bayrak T, Erduran M, Sanscar C, Ekercin S (2012) Remote sensing and GIS-based landslide susceptibility mapping using frequency ratio and analytical hierarchy methods in Rize province (NE Turkey). Environ Earth Sci 66: 2063–2073

Sarkar S, Kanungo DP (2004) An integrated approach for landslide susceptibility mapping using remote sensing and GIS. Photogramm Eng Remote Sens 70(5):617–625

Soeters R, van Westen CJ (1996) Slope instability recognition, analysis and zonation. In: Turner KT, Schuster RL (Eds.) Landslide: investigation and mitigation. Special Report 247. Transportation Research Board, National Research Council, Washington DC, 129–177.

Stocking MA (1972) Relief analysis and soil erosion in Rhodesia using multivariate techniques. Z Geomorphol 16:432–443

Sujatha ER, Rajamanickam V, Kumaravel P, Saranathan E (2013) Landslide susceptibility analysis using probabilistic likelihood ratio model—a geospatial-based study. Arab J Geosci 6(2):429–440

Süzen ML, Doyuran V (2004) Data driven bivariate landslide susceptibility assessment using geographical information systems: a method and application to Asarsuyu catchment, Turkey. Eng Geol 71:303–321

Terzaghi K, Peck RB (1967) Soil mechanics in engineering practice, 2nd edn. Wiley, New York, p 729

Tien Bui D, Pradhan B, Lofman O, Revhaug I, Dick O (2013) Regional prediction of landslide hazard using probability analysis of intense rainfall in the Hoa Binh province, Vietnam. Nat Hazards 66:707–730

Upreti BN, Dhital MR (1996) Landslide studies and management in Nepal. ICIMOD, Kathmandu, p 87

Uromeihy A, Mahdavifar MR (2000) Landslide hazard zonation of the Khorshrostam area, Iran. Bull Eng Geol Environ 58(3):207–213

van Westen CJ (1993). Application of Geographic Information System to landslide hazard zonation. ITC-Publication No. 15, ITC, Enschede, pp. 245

van Westen CJ (1994) GIS in landslide hazard zonation: a review, with examples from the Andes of Colombia. In: Price MF, Heywood DI (eds) Mountain environments and geographic systems. Taylor and Francis Publishers, London, pp 135–165

van Westen C (1997) Statistical landslide hazard analysis ILWIS 2.1 for Windows application guide. ITC Publication, Enschede, 73–84

Varnes DJ (1984) International association of engineering geology commission on landslides and other mass movements on slopes: landslide hazard zonation: a review of principles and practice. UNESCO, Paris, p 63

Vijith H, Madhu G (2007) Application of GIS and frequency ratio model in mapping the potential surface failure sites in the Poonjar sub-watershed of Meenachil River in Western Ghats of Kerala. J Indian Soc Remote Sens 35:275–285

Vijith H, Madhu G (2008) Estimating potential landslide sites of an upland sub-watershed in Western Ghat's of Kerala (India) through frequency ratio and GIS. Environ Geol 55:1397–1405

Wang H, Liu G, Xu W, Wang G (2005) GIS-based landslide hazard assessment: an overview. Prog Phys Geogr 29(4):548–567

Yalcin A, Reis S, Aydinoglu AC, Yomralioglu T (2011) A GIS-based comparative study of frequency ratio, analytical hierarchy process, bivariate statistics and logistics regression methods for landslide susceptibility mapping in Trabzon, NE Turkey. Catena 85:274–287

Yilmaz I (2009) Landslide susceptibility mapping using frequency ratio, logistic regression, artificial neural networks and their comparison: a case study from Kat landslides (Tokat—Turkey). Comp Geosci 35: 1125–1138

Yilmaz I (2010) Comparison of landslide susceptibility mapping methodologies for Koyulhisar, Turkey: conditional probability, logistic regression, artificial neural networks, and support vector machine. Environ Earth Sci 61:821–836

Yilmaz I, Keskin I (2009) GIS based statistical and physical approaches to landslide susceptibility mapping (Sebinkarahisar, Turkey). Bull Eng Geol Environ 68:459–471

Yin KL, Yan TZ (1988) Statistical prediction model for slope instability of metamorphosed rocks. In: Bonnard C (Ed.) Proc 5th Int Sym on Landslides, Lausanne, Switzerland, 1269–1272